Talanta 83 (2011) 1341–1351

Contents lists available at ScienceDirect

Talanta

journal homepage: www.elsevier.com/locate/talanta

Optical supermicrosensor responses for simple recognition and sensitive removal of Cu (II) Ion target

Sherif A. El-Safty*, Adel A. Ismail[1], Ahmed Shahat

National Institute for Materials Science, Exploratory Materials Research Laboratory for Energy and Environment, 1-2-1 Sengen, Tsukuba, Ibaraki 305-0047, Japan

ARTICLE INFO

Article history:
Received 28 September 2010
Received in revised form 28 October 2010
Accepted 1 November 2010
Available online 10 November 2010

Keywords:
Supermicrosensors
Monoliths
Optical detection
Cu(II) ion target

ABSTRACT

The field of optical chemosensor technology demands a simple yet general design for fast, sensitive, selective, inexpensive, and specific recognition of a broad range of toxic metal ions. The suitable accommodation of chromogenic receptors onto ordered porous carriers have led to selective and sensitive chemosensors of target species. In this study, we offer real evidence on the potential use of two- and three-dimensional (2D and 3D) ordered supermicroporous monoliths as selective shape and size carriers for immobilizing the chromogenic probe. Among all the chemosensors, 3D supermicropore has exhibited easy accessibility of target ions, such as ion transports and high affinity responses of receptor-metal analyte binding events. This leads to an optical color signal that is easily generated and transduced even at trace levels of Cu(II) target ions. The supermicrosensors have shown the ability to create Cu(II) ion-sensing responses up to nanomolar concentrations ($\sim 10^{-9}$ mol/dm^3) with rapid response time (in the order of seconds). Supermicrosensors have the ability to create easily modified sensing systems with multiple regeneration/reuse cycles of sensing systems of Cu(II) analytes. The simple treatment using ClO_4^- anion as a stripping agent has removed effectively the Cu(II) ions and formed a "metal-free" probe surface. The supermicrosensors have exhibited the specificity behavior permitting Cu(II) ion-selective determination in real-life samples, such as in wastewater, despite the presence of active component species. Extensive analytical results indicate that the use of the supermicrosensor as Cu(II) ion strips for field screening can be a time- and cost-alternative tool to current effective laboratory assays.

1. Introduction

Beginning the fabrication of classic MS41 materials with pore sizes ranging from 2 to 10 nm by using cationic surfactants [1], significant effort has been expended in creating new levels of hierarchical material designs. These materials exhibit controlled structural geometry, mesophase morphology, pore size, and shape, which can regulate surfactant templates and synthesis conditions [2–7]. Such nanoscale materials have exhibited potential applications in catalysis, separation, biomolecular immobilization, sensing, and optical and electronic technologies [8–10]. Among all possible ordered porous materials, supermicroporous with pores in the 1–2 nm range are of interest because of their advanced functionalities, including size and shape selectivity, accessibility, and retainability of organic molecules with larger sizes than that of zeolites. These conditions result in fine chemical and pharmaceutical development syntheses [8a]. Several fabrication approaches for supermicromaterials have been developed in the past few years [11–14]. Supermicroporous silicas [11,12], organosilicas [13], metal oxides, and phosphates have been fabricated as templates using surfactants and ionic liquids, as well as by employing low temperature synthesis conditions [14]. The potential applications for ordered supermicroporous materials can be widely expanded if they can be fabricated by simple, reproducible synthesis designs into three-dimensional monoliths that have large-particle morphology and well-controlled pore size and shape [10,11].

Chemosensors with selective abilities on specific target cations or anions are very important, given the adverse effects of these toxic ions on human health and the environment [15,16]. Recently, studies have reported that colorimetric sensing systems of metal ions are advantageous for their sensitive and easy signal detection techniques, which do not require sophisticated equipment or well-controlled environment. Sensing responses in terms of sensitivity, selectivity, and fast response-time of chemosensors are induced by receptor "molecular probe"-analyte "cation" interactions [10]. These binding events have employed transduction-signaling responses that pose considerable constraints owing to their chemosensor design. Recently, the advanced functionality of manipulating chromophore probes into nanoscale

* Corresponding author. Tel.: +81 298592135.
E-mail address: sherif.elsafty@nims.go.jp (S.A. El-Safty).
[1] Current address: Nanostructured Materials Lab., Advanced Materials Department, Central Metallurgical R&D Institute (CMRDI), P.O. Box 87, Helwan, Cairo 11421, Egypt.

0039-9140/$ – see front matter © 2010 Elsevier B.V. All rights reserved.
doi:10.1016/j.talanta.2010.11.008

materials as sensing receptors has received wide attention (i.e., flexible chemosensor designs) due to their responsive recognition of several species like metal cations [17,18], as well as charged and neutral organic molecules [19]. However, new porous chemosensing schemes still demand pore dimensional materials in order to control the shape selectivity of molecular recognition "probe" units; in turn, this generates signal transduction as a response of the binding event [20].

Due to its environmental and biological importance, the development of optical chemosensors for simple detection of Cu(II) ions has been particularly crucial among researchers [21,22]. Cu(II) ion is one of the target metal ions used as a micronutrient element in mammalian nutrition. Both deficient and excessive intake of this ion by human and animal bodies from food, water, air, and others, might cause various symptoms like vomiting, lethargy, acute hemolytic anemia, renal and liver damage, neurotoxicity, and increased blood pressure and respiratory rates [23,24]. With the common use of Cu(II) target ions in various industries and biological treatments, numerous techniques have been developed for detection of Cu(II). Extensive techniques like extractive atomic absorption spectrometry [25], spectrophotometry [26], atomic absorption spectrometry [27], inductively coupled plasma-atomic emission spectroscopy [28], stripping voltammetry on a mercury drop [29], differential pulse anodic stripping voltammetry [30], X-ray fluorescence [31], and atomic fluorescence spectrometry have been developed to detect Cu ions [32]. These techniques have lead to improved monitoring from the perspective of precision, accuracy, sensitivity, and selectivity, but they have also been restricted by preconcentration procedures and generation of organic wastes. The potential of such methods is also limited by high investment cost, complexity, and difficulty in in situ application. Meanwhile, optical chemosensors have been developed as well for detecting Cu ions. One such case is the modified fluorophore surface sensor, which can emit fluorescence that can be used for detecting and analyzing Cu(II) ions [15g,21h,33,34]. Moreover, the detection of Cu^{2+} ion using electrochemical sensors based on attenuated internal reflectance stripping voltammetry has been reported [35]. Changes in absorption spectra in the ultraviolet-to-near infrared region have been used to trigger analytical signals by modifying suitable receptor ligands onto the optical sensors of Cu(II) ions [36]. However, despite these successes, most of these methods require intensive conditions, well-controlled equipment, and lengthy and time-consuming assessments, which make them unattractive candidates for significant detection of Cu(II) analytes [37]. Accordingly, the need for chemosensors that integrates simplicity and flexibility in the fabrication design, but which retains selective and sensitive determination of toxic ions, has become a focal interest in the chemical sensor field [15–23,36,37].

We have recently reported chemosensor designs for several metal ions based on the integration of organic chromophores into these functionalized mesoporous silica monoliths. Such systematic designs have led to the anchoring of organic dyes into 3D inorganic networks with well-defined cage cavities and unique properties [18]. These nanosensor designs has allowed for naked-eye detection of metal ions up to nanomolar concentrations. However, the practical applicability of such nanosensors still depend on the nanoscale materials and their physical properties, as these can enhance the sensitivity and response time of metal-to-ligand binding during recognition processes [18,19]. In this paper, the potential functionality of 2D hexagonal MCM-41 and 3D cubic *Fd3m* (HOM-11) supermicroporous monoliths acting as size- and shape-selective carriers for accommodating hydrophobic chromophore probes (with molecular size ≤ 1.4 nm), such as dithizone (DZ), is revealed. For the first time, the design of the chemosensor based on supermicropore carriers has enabled the visual detection of ultra-traces of toxic Cu(II) ions. DZ-probes are commonly used as indicators for selective detection of Cu(II) analytes up to 10^{-6} mol/dm^3 in a solution. DZ-doped supermicropores could also be used as preconcentrators for simple separation and simultaneous detection of toxic Cu(II) analytes, but less the use of sophisticated instruments. A key advantage in employing supermicrosensors is the ability to create sensing system responses with revisable, selective, and sensitive recognition using naked-eye detection of Cu(II) target ions up to nanomolar concentrations ($\sim 10^{-9}$ mol/dm^3) with rapid kinetic assessments (in the order of seconds).

2. Experimental

All materials were used as produced without further purification. Diphenylthiocarbazone (dithizone, DZ), tetramethylorthosilicate (TMOS), decane (C_{10}-alkane), dodecyltrimethylammonium bromide (C_{12}TMAB) surfactant, and Cu(II) standard solution were obtained from Wako Company Ltd. (Osaka, Japan). Buffer solutions of either 0.01 M sulfuric acid or 0.2 M KCl–HCl, and CH_3COOH–CH_3–COONa were used to adjust the pH in the 1–6 range. A mixture of 2-(cyclohexylamino) ethane sulfonic acid (CHES), 3-morpholinopropane sulfonic acid (MOPS), and N-cyclohexyl-3-aminopropane sulfonic acid (CAPS) was used to adjust the pH in the 7–11 range by using 0.2 M NaOH.

2.1. Synthesis of hexagonal MCM-41 and cubic Fd3m supermicropore monoliths

Supermicroporous hexagonal *P6mm* (MCM-41) and cubic *Fd3m* (HOM-11) monoliths were fabricated via an instant direct-template methods using both lyotropic and microemulsion systems of cationic surfactant (C_{12}TMAB) at C_{12}TMAB/TMOS ratio of 50 wt% used as templates [7]. The addition of long chain alkanes ($\geq C_{10}$-decane) to the hexagonal mesophase led to both the diameter and surface interfacial curvature of (C_{12}TMAB) micelles that were increased under instant synthesis conditions. Therefore, the cubic *Fd3m* mesophase could be formed in this microemulsion system [7].

The conditions and procedure in the synthesis of translucent cubic *Fd3m* monoliths at a specific C_{12}TMAC/TMOS ratio of 50 wt% in the microemulsion system is as follows: first, 1 g of cationic surfactants, 0.5 g of decane (C_{10}-alkane), and 2 g TMOS were mixed in a flask to yield a milky solution. Then, 1 g of H_2O/HCl (pH = 1.3) was quickly added to form a clear solution (i.e., homogenous). The mass ratio of C_{12}TMAB:decane:TMOS:H_2O/HCl was 1:0.5:2:1. For all syntheses of MCM-41 and HOM-11 mesophases, the lyotropic and microemulsion composition mixture domains were not aged (i.e., without static condition while mixing). The methanol produced from the TMOS hydrolysis was removed by a diaphragm vacuum pump connected to a rotary evaporator at 40–45 °C. After ~5 min, an optical gel-like solid was formed, acquiring the shape and size of the reaction vessel. To obtain centimeter-sized, crack-free, and shape-controlled supermicroporous silica monoliths, the resultant translucent cationic surfactants/silica solid was gently dried at room temperature for 3 h and allowed to stand in a sealed container at 25 °C for 1 d to complete the drying process. The organic moieties were then removed by calcination at 450 °C for 7 h [7].

2.2. Fabrication design of 2 and 3D supermicrosensors

Chemosensors with 2 and 3D supermicroporous were fabricated by using direct immobilization of the ethanol solution of 10 mg DZ-probe into 0.5 g hexagonal *P6mm* and cubic *Fd3m* supermicropore carriers. The ethanol was removed by gentle vacuum connected to a rotary evaporator at room temperature, leading to the direct intact of the dye probe into the supermicropore silicas.

Table 1
Cu(II) ion-sensing responses of the design-made supermicrosensors with 3D cubic *Fd3m* and 2D hexagonal MCM-41 monolithic geometries.

Supermicro-sensor geometry	Q (mmol/g)	$10^9 \times L_D$ (mol dm^{-3})	$10^8 \times L_Q$ (mol dm^{-3})	D_R (mol dm^{-3})	t_R (s)	Regeneration cycles		
						No.	E (%)	t_R (s)
3D Fd3m	0.036	31	105	$1.57 \times 10^{-8} - 7.86 \times 10^{-6}$	60	2	98	70
						4	97	80
						6	95	100
2D MCM-41	0.03	125	416	$7.86 \times 10^{-8} - 7.86 \times 10^{-6}$	80	2	97	100
						4	95	120
						6	93	150

Adsorption amount (Q) of the DZ-probe molecules at saturation step, limit of detection (L_D) and quantification (L_Q), detection range (D_R), and response-time (t_R). The ion-sensing efficiency (E) of the supermicrosensors within the recycle numbers was estimated in terms of the sensitivity during the detection of Cu(II) ions.

The immobilization process was repeated several times until the equilibrium adsorption capacity of DZ probe reached saturation. The resulting supermicroporous sensors were thoroughly washed with deionized water until no elution of DZ color was observed. The chemosensors were dried at 65 °C for 2 h. The adsorption capacity (Q, mmol g^{-1}) of the DZ probe at saturation was determined by the following equation: $Q_t = (C_o - C_t)\,V/m$, where Q_t is the adsorbed amount at saturation time t, V is the solution volume (L), m is the mass of HOM carriers (g), C_o and C_t are the initial concentration and the concentration at saturation time, respectively (see Table 1). *Note*: the stoichiometry of [M-DZ] complexes was derived from the deviation from linearity at the inflection point in the calibration curve, the M:DZ stoichiometric ratio of the $[Cu\text{-}DZ]^{n+}$ complexes were 1:2 using 2 and 3D supermicroporous chemosensors. Further evidence of the stoichiometric $[Cu\text{-}DZ]^{n+}$ complexes was seen in the Job's plot in which changes in the absorbance of the color complexes in solution under experimental control conditions were monitored. Results indicated no changes in the stoichiometry of the $[Cu\text{-}(DZ)_2]^{n+}$ complexes formed in both homogeneous and heterogeneous systems.

2.3. Analyses of ultra-traces level of Cu(II) ions

The colorimetric determination and visual detection of Cu(II) analyte by using DZ probe-doped supermicroporous chemosensors were carried out by adding a mixture containing specific concentrations of each analyte ions adjusted at pH ca. 2 (by using 0.2 M of KCl/HCl/H_2SO_4), pH 4 (by using 0.2 M CH_3COOH/CH_3-COONa), and pH 7 (by using 0.2 M of 3-morpholinopropane sulfonic acid, MOPS), respectively, to ~4–5 mg of the supermicroporous sensor monoliths at constant volume (20 cm^3) with shaking. After an interval of time, the supermicroporous solid chemosensors were collected by using suction and 25-mm-diameter cellulose acetate filter paper (Sibata filter holder). The color of the collected sample was estimated by the naked-eye and UV–vis spectrometry. In order to quantitative record the change in the color of the sensors by addition of the Cu(II) ions using solid-state UV–vis spectrophotometer, the solid monolithic sensors were grinded to fine powder disc to observe the homogeneity in the reflectance spectra. Our previous studies revealed that the monolith-based sensor in the grinded form did not loss its utility or functionality in terms of fast response-time and sensitivity [18b]. The concentration of Cu(II) ions was analyzed by using a Seiko SPS-1500 inductively coupled plasma atomic emission spectrometer (ICP-AES) before and after detection. To ensure both accuracy and precision of the analyte ion sensing system, successive measurements were carried out using wide-range concentrations of the standard "well-known" solutions of analyte ions. The reflection intensities of the $[Cu\text{-}(DZ)_2]^{n+}$ complexes formed by using both the standard solutions and target samples were compared to estimate the $[Cu^{2+}]$ analyte ions. The detection and quantification limits (L_D and L_Q) of Cu(II) analyte ions by using the supermicroporous chemosensors was estimated from the linear part of the calibration plot [18a,b], according to the equation L_D and $L_Q = k_{1,2}S_b/m$, where $k_1 = 3$ and $k_2 = 10$ in case of the determination of detection and quantification limits, respectively, S_b is the standard deviation for the blank, and m is the slope of the calibration graph in the linear range. In addition, the stability constant ($\log K_s$) of the formed $[Cu\text{-}(DZ)_2]^{n+}$ complex into the nanosensors at pH 2 was estimated as 7.2, according to the following equation: $\log K_s = [ML]_S/[L]_S \times [M]$; where [M] refers to the concentration of Cu(II) ions in solution that have not reacted with the DZ chelating agent, [L] represents not only the concentration of free DZ ligand but also all concentrations of DZ not bound to the Cu(II) ion, and the subscript S refers to the total concentration and the species in the solid phase.

2.4. Instruments

The reflection spectra of the supermicroporous chemosensors were recorded using by a Shimadzu 3700 model solid-state UV–vis spectrophotometer. Small-angle powder X-ray diffraction (XRD) patterns were measured by using a 18 kW diffractometer (Bruker D8 Advance) with monochromated CuKα radiation with scattering reflections recorded for 2θ angles between 0.1° and 6.5° corresponding to d-spacings between 88.2 and 1.35 nm. N_2 adsorption–desorption isotherms were measured using a BELSORP MIN-II analyzer (JP. BEL Co., Ltd.) at 77 K. The pore size distribution was then determined from the adsorption curve of the isotherms by using nonlocal density functional theory (NLDFT). Transmission electron microscopy (TEM) was operated at 200 kV electron microscope (JEOL 2000 EX II) which has a point-point resolution of 0.21 nm and a spherical aberration of 0.7 nm. Fourier transform diffractograms (FTD) patterns were recorded from by a slow scan charge-coupled device (CCD) camera (Gatan Model 694). Scanning electron microscopy (SEM) was measured by a field-emission scanning electron microscopy (Hitachi S-4300) that operated at 20 keV.

3. Results and discussion

3.1. Design of 2D and 3D supermicrosensors

A particularly important feature of the 2D and 3D supermicroporous monoliths fabricated in this study was the potential size and shape selectivity for the DZ-probe (molecular size ≤ 14 Å). In particular, the 3D cubic *Fd3m* supermicroporous carriers were twice higher in accessibility and adsorption capacity (Q) at 0.036 mmol/g compared with that of synthesized 2D mesoporous hexagonal P6mm (SBA-15 and MCM-41). 3D cage and cylindrical cubic monoliths exhibited large pores (~10 nm), as well as mesopore and micropore volumes (~2.0 and 0.2 cm^3/g, respectively) [18,19]. The high adsorption capacity of DZ-probe in a similar pore size of supermicroporous monoliths is indicative of the effective use of

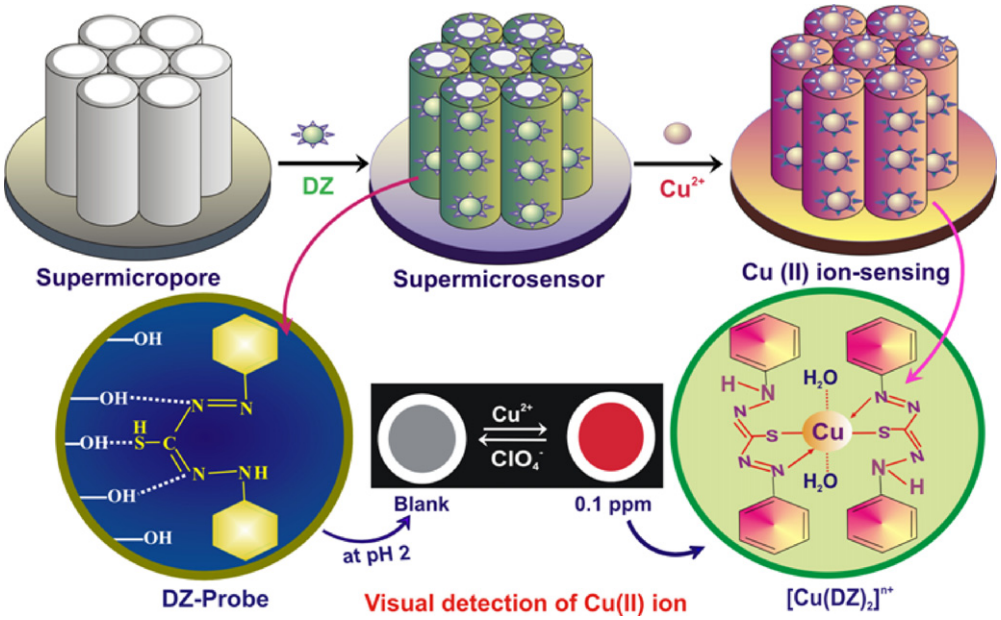

Scheme 1. Systematic design-made supermicrosensors through the direct immobilization of DZ-probe onto 2D hexagonal MCM-41 supermicropore monoliths. The enlarged section inside the supermicropores exhibited possible formation of the $[Cu\text{-}(DZ)_2]^{n+}$ complex and the analytical reuse cycle in these sensing responses during the visual detection of Cu(II) ion at pH 2. The scheme revealed the possibility of using regular supermicropores as selective shape and size carriers for the DZ-probe receptor.

supermicropores as size- and shape-selective carriers in accommodating hydrophobic chromophore probes. These supermicroporous monoliths gave high responses during the sensing assays of Cu(II) ions. Moreover, the physical adsorption of the DZ-probe into supermicroporous carriers led to the control design of 2D and 3D supermicrosensors [18]. However, the interaction between hydroxyl groups of supermicropore silicas and heteroatoms of DZ-probe not only led to the retention of the DZ-probe into the supermicropores, it also enhanced the required flexibility of the [DZ-metal] binding events (Scheme 1). This resulted in the efficient signaling response of the supermicrosensors for visual detection of Cu(II) ions (Table 1). The high surface area, shape and size selectivity, and large particle-size grains of the HOM supermicroporous monoliths are advantageous for the high adsorption capacity of the DZ-probe in fast adsorption kinetics [17–20].

Supermicrosensors have well-organized pore arrays (Fig. 1A) despite their high accessibility of DZ-probe into supermicropore surfaces. XRD patterns of supermicropore carriers and sensors (Fig. 1A) revealed well-defined diffraction peaks, which were consistent with hexagonal MCM-41 face-centered cubic *Fd3m* structures. In general, TEM and FTD patterns can reveal the retention of uniformly shaped hexagonal *P6mm* (Scheme 1) and cubic *Fd3m* (Fig. 2) supermicropore geometries of DZ-modified supermicrosensors. The N_2 isotherms (Fig. 1B) exhibited well-defined capillary condensation at $0.08 \leq P/P_o \leq 0.18$ of isotherms between type I and IV curves, indicating uniformly sized pore of less than 2 nm (Fig. 1B, insert). This was well in agreement with TEM profiles (Fig. 1B) [11–14]. The decrease in supermicropore size, surface area, and pore volume correspond to the inclusion of DZ-probe molecules into supermicropore carriers. This result mainly

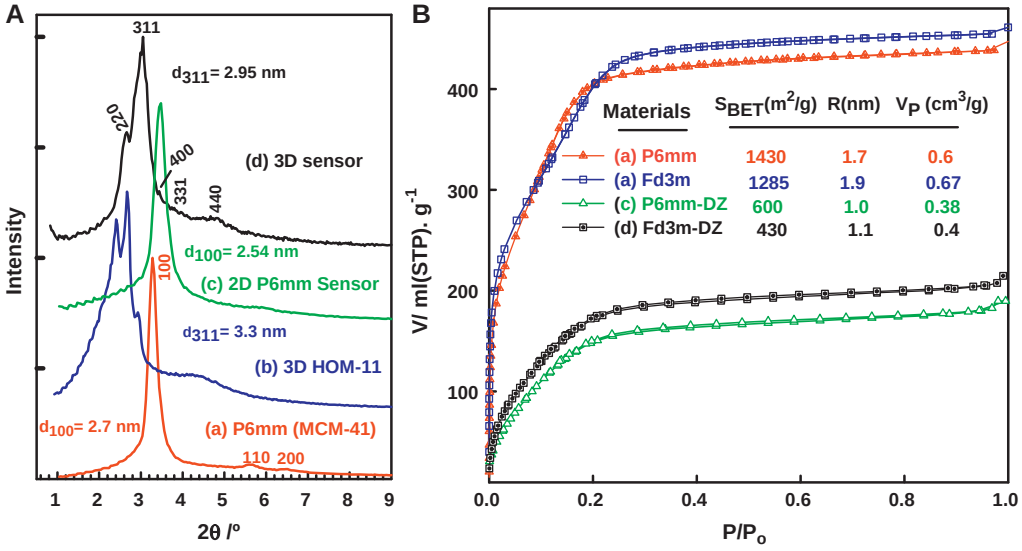

Fig. 1. XRD patterns (A) and N_2 adsorption/desorption isotherms at 77 K (B) of supermicroporous monoliths (a and b) and sensors (c and d) with highly ordered hexagonal P6mm (MCM-41) and cubic Fd3m (HOM-11) structures.

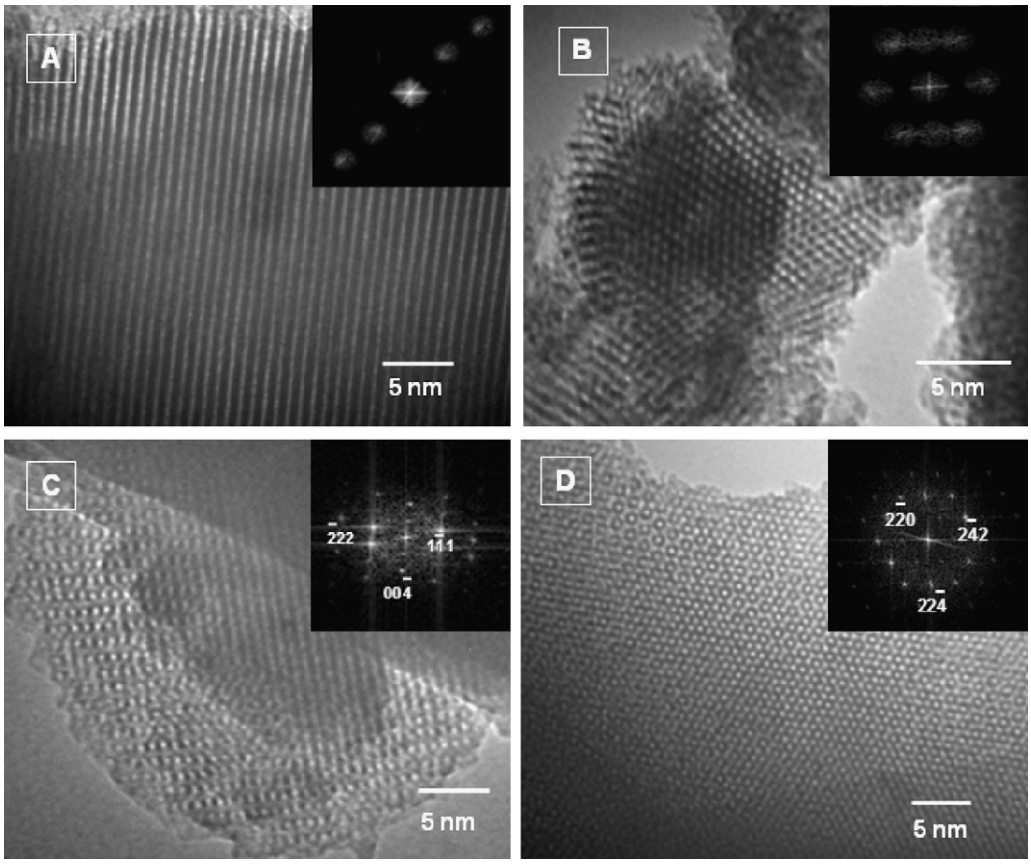

Fig. 2. Representative TEM images of ordered supermicrosensors fabricated by immobilization of DZ-probe onto (A and B) hexagonal P6mm (MCM-41) and (C and D) cubic Fd3m monolithic carriers (HOM-11) recorded along (c) [1 0 0] and (d) [1 1 0].

indicates that the DZ-probe has become a rigid part in inner supermicropore surfaces [18]. In addition, the retention of the physical characteristics of the supermicrosensors (Fig. 1B, insert) could enhance the diffusion kinetics for DZ-Cu analyte binding events, as evidenced by the fast response time (in the order of second), even with the recognition of low concentration Cu(II) analyte (Table 1).

The supermicrosensor monoliths have micrometer-sized particles (Fig. 3). The crystal particles of these monolith supermicrosensor predominantly revealed plate-like particles with smooth fine lines on their surface morphology. SEM micrographs (Fig. 3A and B) showed morphological defects, such as dense macroporous voids (open holes). The grain sizes of these morphological defects were not uniform (between 1 and 5 μm) and were shaped irregularly. The formation of large morphological particles and macroporous pores of supermicrosensor materials might have enabled adsorption of a large number of DZ-probe in the pore wall surfaces with flexible and reasonable orientation during the binding of Cu(II) ion targets, as evidenced from the fast response time (within seconds).

3.2. Supermicrosensors for Cu(II) ion-sensing systems

The quantification procedure of Cu(II) ion-sensing with 2D and 3D supermicrosensors was studied after equilibration time or response time (t_R). The prominent color change and signal satura-

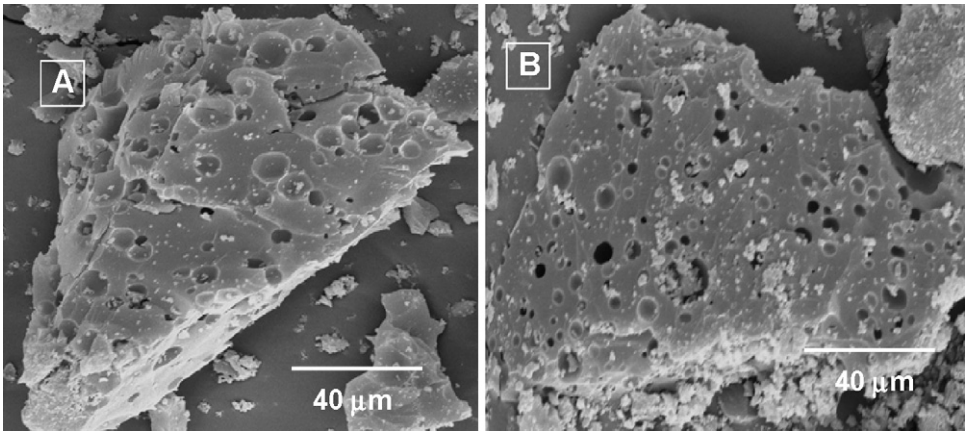

Fig. 3. Representative SEM images of ordered supermicrosensors fabricated by immobilization of DZ-probe onto (A) hexagonal P6mm (MCM-41) and (B) cubic Fd3m monolithic carriers (HOM-11).

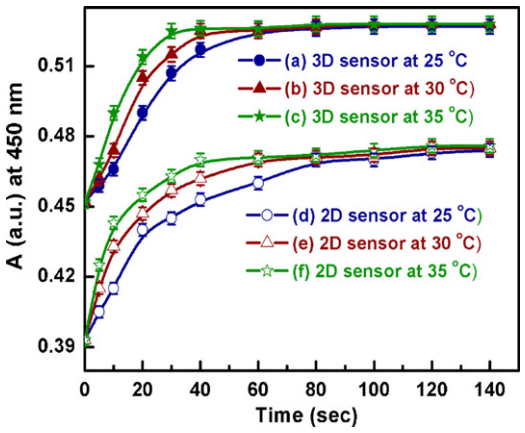

Fig. 4. The kinetic time-dependence and the temperature (25–35 °C range) effects on the UV/vis reflectance spectra of Cu(II)-to-DZ ligand binding responses during the recognition of [7.87 μM] Cu(II) ions using 4.0 mg of 3D and 2D supermicrosensors at pH 2 and volume of 20 mL. The error bars are ≤1% for all analytical data.

tion in the reflectance spectra of supermicrosensors are shown in Fig. 4. This response-time could be considered as a reference signal with practically no Cu(II) analyte ion retention, as evidenced by the equilibration time of the S-shape curve at different ion-sensing temperatures (Fig. 4). The fast Cu(II)-to-ligand binding kinetics of the $[Cu\text{-}(DZ)_2]^{n+}$ complex formation was studied by monitoring continuously the UV/vis reflectance spectra of the supermicrosensors after adding Cu(II) ions; data were then used as a function of time at optimal sensing conditions (i.e., pH of 2, sensor amount of 4 mg, and volume of 20 mL) (Fig. 4). The charge transfer between Cu(II) ions and DZ-probe occurred within a short time period (~60 s) due to the ability of the DZ-probe chemosensors to have open and uniformly shaped supermicropore architectures, which allowed for the efficient binding of metal ions. Despite the presence of either low or high concentration of Cu(II) ions for the sensing responses, no significant change in the response time of the chemosensors was evident, indicating high availability and affinity of the DZ-probe ligand for Cu(II) ion binding at a wide range of Cu(II)-ion concentrations. As shown in Fig. 4, an increase in solution temperature can significantly influence the Cu(II) ion-sensing rate of supermicrosensors. In addition, the t_R value was extended to ~80 s when 2D MCM-41 supermicrosensors were applied to the visual detection of Cu(II) ions. The high metal flux (ion transport) and affinity of the metal-ligand binding were significantly affected by ion-sensing temperature, 3D shape, and geometry of supermicrosensors, as clearly evidenced by the t_R value (Table 1) [18,19].

The successful immobilization of DZ-probe onto the shape- and size-selective supermicropore carriers has led to the design of chemosensors capable of accurately detecting Cu(II) analytes up to nanomolar concentration. High performance 2D and 3D supermicroporous chemosensors [i.e., in terms of sensitivity and kinetic reaction between Cu(II) ions and DZ-probe ligand (response-time, t_R) depended on key components such as pH value (Fig. 5) and amount of solid-based sensor (Fig. 5) [15–19]. Changes in these experiment controls could significantly affect sensing responses of the supermicrosensors. In this study, we carried out a series of experiments to systematically define and evaluate suitable conditions for the donor-acceptor combinations between DZ-probe and Cu(II) analyte. With different Cu(II) ion concentrations, the optimum change in the color intensity of the $[Cu\text{-}(DZ)_2]^{n+}$ complex was around pH 2. The pH graph suggests that the Cu(II) ion can bind strongly to DZ-probe with high binding constant ($\log K_s = 7.2$) during the formation of $[Cu\text{-}(DZ)_2]^{n+}$ complex at pH 2. Scheme 1 shows the most probable structure of Cu-DZ chelate complex.

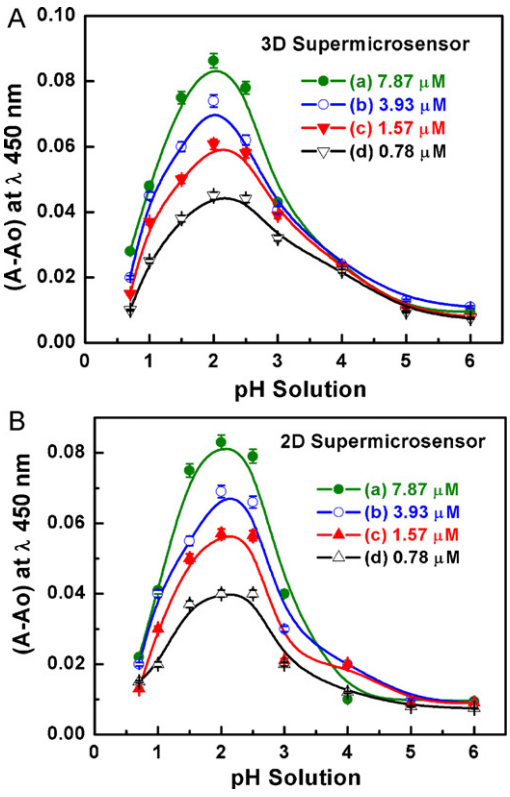

Fig. 5. Quantitative study of pH supermicrosensor responses during the recognition of different concentrations (0.78–7.87 μM) of Cu(II) ions at optimal sensing conditions (t_R > 1 min, supermicrosensor amount of 4 mg, volume of 20 mL, and temperature of 25 °C). The error bars are 2.5% for all analytical data.

Within the Cu(II) ion-sensing system, the nature of the complex formation and its stability was also dependent on the adsorption amount of DZ-probe onto supermicropore carriers. The amount of 2D and 3D supermicrosensor solids significantly affected the Cu(II) ion sensing utility (Fig. 6). Fig. 6 shows that 4 mg of 2D and 3D solid HOM-DZ supermicrosensors was sufficient to achieve good color separation "signal" between the supermicrosensor "blank" and the Cu(II) ion-sensing "sample" even at low recognition of trace-level of Cu(II) concentration. The color intensity of the $[Cu\text{-}(DZ)_2]^{n+}$ complex depended on the amount of solid chemosensor and the structural geometry of the supermicrosensors. In the solid-state ion-sensing system, the sensitivity of chemosensor strongly

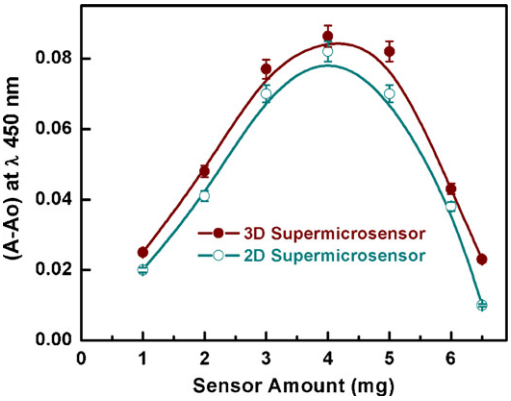

Fig. 6. The effect the amount of solid sensor on the UV/vis reflectance spectroscopic responses of $[Cu\text{-}(DZ)_2]^{n+}$ complex during the recognition of [7.87 μM] Cu(II) ions at optimal sensing conditions (volume of 20 mL and temperature of 25 °C). The error bars are 2.5% for all analytical data.

depended on the adsorbed amount of probe onto pore surfaces of the carriers (Table 1) [18].

3.3. Visual detection of ultra-traces Cu(II) ions

The DZ receptor was used for the sensitive determination of Cu(II) analyte ions in the solution by up to 10^{-6} mol/dm^3 [37]. Apart from their capability to function as chemosensors, DZ-doped supermicroporous carriers could also be used as preconcentrators in order to yield high adsorption capacity and preconcentration efficiency. The utility of the design-made supermicroporous-DZ receptor led to simple separation and visual detection over a wide, adjustable range, as well as the sensitive quantification of analyte ions at trace levels ($\sim 10^{-9}$ mol/dm^3). No elution of the DZ-probe was evident upon adding Cu(II) analyte ions during the sensing responses. The rapid and flexible Cu-DZ binding events onto supermicrosensors led to the separation and preconcentration of Cu(II) ions even at trace concentration levels. The color change provided a simple procedure for sensitive and selective detection of Cu(II) ions without the need for sophisticated instruments (Scheme 1) [38–40].

The design-made chemosensor with 3D ordered cubic *Fd3m* geometry showed higher potential signal as a response to Cu(II)-DZ ligand binding events compared with that of 2D hexagonal chemosensors (Table 1). The 3D functionality and connectivity of the cubic *Fd3m* supermicroporous carriers might have been the cause of the fast accessibility of Cu(II) analytes and ion transports (Fig. 4), and high affinity binding events, as clearly evidenced by significant naked-eye sensing ability, particularly at trace levels of Cu(II) target ions (Table 1). Clearly, 3D supermicropore geometries play a role in the design of an efficient and sensitive sensing system of toxic Cu(II).

The UV–vis absorption of DZ-probe receptors in the solution showed strong Cu-to-ligand charge transfer band at 480 nm with the addition of Cu(II) target ions at the constant pH of 2 and 25 °C [37]. Cu(II) quantification experiments were carried out on a quartz flask with a total volume of 25 mL. The absorption intensity of the $[Cu\text{-}(DZ)_2]^{n+}$ complex (data not shown) heightened with the increase in concentration of the Cu(II) ions from 8.9×10^{-7} to 1.57×10^{-5} mol/dm^{-3}. A key to the success of the design-made supermicrosensors was that the colorimetric determination by using UV–vis reflectance spectroscopy have validate quantitatively the wider concentration range of the metal ions (1.57×10^{-8} to 7.86×10^{-6} mol/dm^3) compared with the metal ion recognitions in solution. The signaling change in the reflectance spectra of chemosensors was monitored during the $[Cu\text{-}(DZ)_2]^{n+}$ complex formation (Fig. 7). The reflectance spectra of the supermicrosensors exhibited a blue shift from (λ_{max}) 596 to 450 nm as a result of the binding of Cu(II) target ions with the DZ-probe ligand (Fig. 7). The signaling responses indicate the formation of charge-transfer $[Cu\text{-}(DZ)_2]^{n+}$ complexes. Results from the binding constant of $[Cu\text{-}(DZ)_2]^{n+}$ complex suggest further that sulfur- and nitrogen-chelating groups of DZ ligand have tightly combined with Cu(II) ions in the typically octahedral $[Cu\text{-}(DZ)_2]^{n+}$ complex formation at a pH of ~2 (Scheme 1).

The calibration plot of the 2D and 3D DZ-probe supermicrosensors can be presented as a linear correlation at low concentration ranges of Cu(II) analyte ions (Fig. 8). Specifically, the linear curves indicate that the Cu(II) analyte can be detected with high sensitivity over a wide range of concentrations. However, a non-linear correlation at the inflection point was evident at the highest Cu (II) ion concentration ($\geq 2.0 \times 10^{-6}$ M). The quality of the calibration methods was necessary in ensuring both accuracy and precision of the Cu(II) ion sensing systems. Several quantification measurements (≥10 times) were carried out using a wide range of concentrations (1.57×10^{-8} to 7.86×10^{-6} M) from among standard "well known" solutions of Cu(II) ions under specific sensing conditions. The standard deviation for the analysis of Cu(II) ions using supermicrosensors was of 1–5%, as shown in the fitting plot of the calibration graphs (Fig. 8, inserts). The quantification limit (L_Q) corresponds to the precise correlation of our experimental sensing procedure, as evidenced by the Cu (II) ion-sensing data obtained from fabricated nanosensors (Table 1). Furthermore, the design-made supermicroporous chemosensors enabled

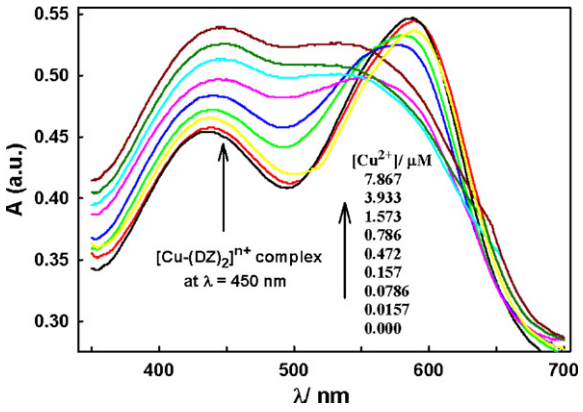

Fig. 7. Concentration-dependent changes in UV/vis reflectance spectroscopic responses of 3D supermicrosensors during the recognition of Cu(II) analyte ions at optimal sensing conditions (pH of 2, $t_R > 1$ min, supermicrosensor amount of 4 mg, volume of 20 mL, and temperature of 25 °C).

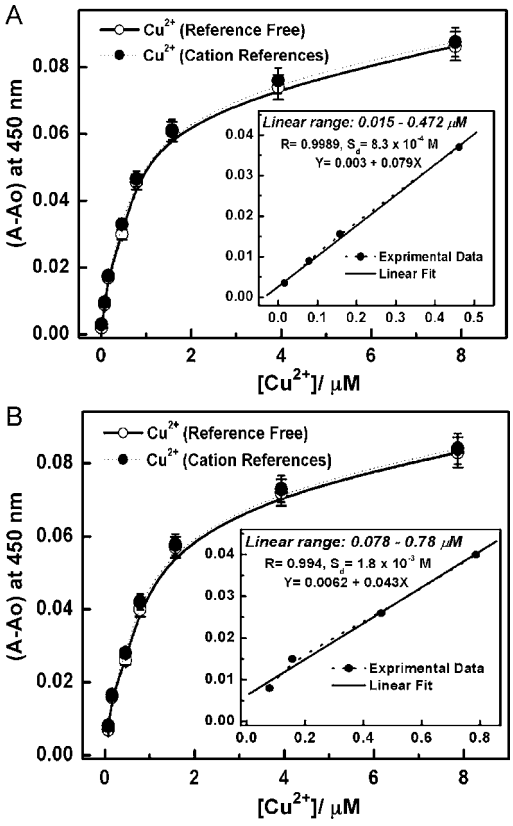

Fig. 8. Representative calibration curve ($A - A_o$ and [Cu(II)] concentration, where A_o and A_c is the absorbance of DZ-probe and $[Cu\text{-}DZ]^{n+}$ complex at λ = 450 nm) of 3D (A) and 2D (B) supermicrosensors during the recognition of Cu(II) ion (in the absence of interferences, see solid line) and in the addition of interfering cations (see dotted line) with high concentration. The inlet shows the amplification for the low-limit colorimetric response to Cu(II) ions (experimental data). The graph is represented by a linear fit line in the linear concentration range before saturation. The error bars denote a relative standard deviation of 1–5% for analytical data in 10 replicates.

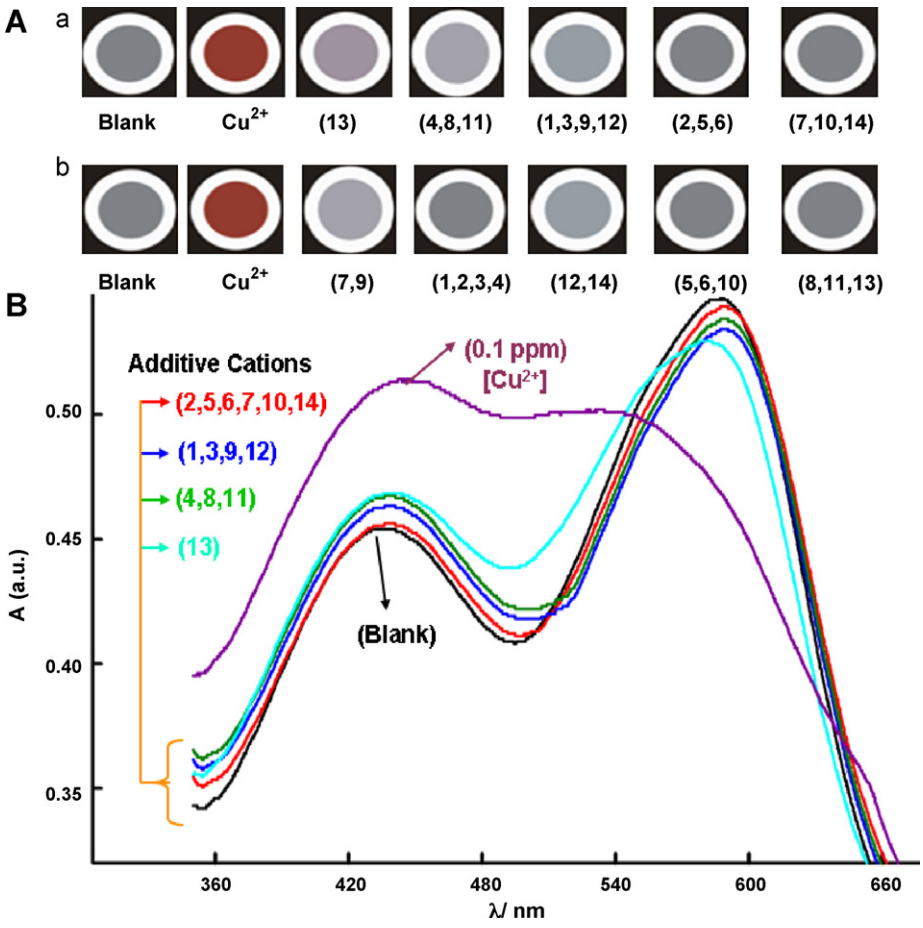

Fig. 9. Color profiles (Aa and Ab) and UV/vis reflectance spectra (B) of the 3D supermicrosensors (blank) during the addition of various foreign cations (a), anions and surfactants (b), and 0.1 ppm of Cu (II) ion. The cations listed in order (1–14) 20 ppm Ni^{2+}, 15 ppm Co^{2+}, 10 ppm Al^{3+}, 5 ppm Fe^{3+}, 50 ppm Ca^{2+}, 50 ppm Mg^{2+}, 15 ppm Zn^{2+}, 10 ppm Hg^{2+}, 15 ppm Pb^{2+}, 15 ppm Cr^{3+}, 10 ppm Sb^{3+}, 20 ppm Cd^{2+}, 15 ppm Bi^{3+}, and 10 ppm Mo^{6+}. The surfactants and anions listed in the order (1–14), 20 ppm SDS, 35 ppm CTAB, 50 ppm Triton X100, 50 ppm $C_8H_4O_4^{2-}$, 50 ppm $C_6H_5O_7^{2-}$, 50 ppm $C_2O_4^{2-}$, 15 ppm Cl^-, 15 ppm CH_3COO^-, 5 ppm NO_2^-, 20 ppm NO_3^-, 20 ppm SO_3^{2-}, 20 ppm SO_4^{2-}, 25 ppm PO_4^{3-}, and 30 ppm CO_3^{2-}. Sensing signal responses of cation and anion species are obtained at pH 2 after 60 s of contact. The experiments are performed at 25 °C with overall volume maintained at 20 mL.

the possible detection limit (L_D) of these target ions to reach sub-nanomolar concentrations despite the simplicity of this sensing system (Table 1). The shape- and size-selective supermicropore sensors can effectively separate and preconcentrate the Cu(II) ions at trace concentrations.

3.4. Reversible Cu(II) ion-sensing system

A key component of the 2D and 3D supermicrosensors is the ability to create easily modified sensing systems with multiple regeneration/reuse cycles for the Cu(II) analytes sensing system [15–20,40,41]. The ClO_4^- anion, which was used as the stripping agent at 0.1 mol/L concentration, could effectively remove the Cu(II) ions (i.e., decomplexation) (Scheme 1). ClO_4^- as an eluant have higher binding affinity in forming stable Cu(II) complexes compared with that of Cu(II)-DZ-probe complexes. We have carried out these experiments several times via liquid-exchange process in order to release the Cu(II) ions and to obtain a "metal-free" probe surface. UV–vis spectroscopic studies were substantially conducted for the supermicrosensor (blank) after decomplexation in order to investigate the stability of the DZ-probe onto the solid monoliths. In order to investigate the efficiency of the sensor design (E), after several times (No.) of regeneration cycle, the signal intensity of the $[Cu\text{-}(DZ)_2]^{n+}$ complex formation with each reuse cycle was compared with the signal spectra of the sensor prior the use of ClO_4^- (Table 1). After multiple regeneration/reuse cycles (i.e., $\geq$6), the $[Cu\text{-}(DZ)_2]^{n+}$ complex showed well-controlled signaling in the quantification and detection of Cu(II) ions. However, the Cu(II) ion-sensing systems with regenerated supermicrosensors slightly influenced sensitivity with increased recovery time (t_R) of Cu-to-DZ ligand binding (Table 1). The effective binding and signaling of the metal ion targets to the electron acceptor/donor strength of the DZ-probe functional sites were significantly degraded because of the substantial influence of the regenerating agent upon cycling and recycling. The 2D and 3D supermicrosensors remained effective even after extended sensing and regeneration cycles. The supermicrosensors showed similar reversibility as that of nanosensors for metal ion sensing systems [18,19].

3.5. Cu (II) ion-selective supermicrosensors

Even with the addition of active component species, the DZ-probe supermicrosensors exhibited specificity behavior that permitted selective determination of Cu(II) ions (Fig. 9 and Table 2). Such interfering species would often hinder the sensing systems of these analytes [18,38–41]. In order to determine the competing effects of interfering cations and anions in the Cu(II) ion-selective supermicrosensors, two key methods were applied (pH of 2, t_R > 1 min, sensor amount of 4 mg, volume of 20 mL, and temperature of 25 °C). First, a series of transition and groups (I and II) of metal ions and anionic interferences were tested individually with supermicrosensors. A high concentration at 5–5000 ppm range was

Table 2
The tolerance limit (T_L) of the additive matrix species and the stability constant ($\log K_s$) of the [Cu-$(DZ)_2$]$^{n+}$ complex formation during addition of high concentration of interfering species to 3D optical supermicrosensor system prior to the recognition of [0.1 ppm] Cu(II) target ions at the specific conditions (pH of 2, t_R > 1 min, sensor amount of 4 mg, volume of 20 mL, and temperature of 25 °C).

Common electrolyte species (ppm)											
Matrices	KNO_3	F^-	NaCl	SO_4^{2-}	NaBr	NO^{2-}	CO_3^{2-}	IO_3^-	SO_3^{2-}	SCN^-	PO_4^{3-}
T_L	5550	375	5000	20	1000	30	30	50	20	98	25
Log K_s	7.2	7.202	7.1	7.16	7.2	7.17	7.2	7.2	7.204	7.22	7.205

Surfactants and complexing agents (μM)											
Matrices	CTAB	TAAC	TEAC	DDAB	SDS	TX	Oxal.	Citr.	Tart.	Phth	Acet.
T_L	40	40	45	35	20	50	55	50	60	65	45
Log K_s	7.203	7.204	7.202	7.203	7.21	7.2	7.2	7.23	7.24	7.22	7.2

Foreign cations (ppm)															
Ions	Cr (III)	Fe (III)	Mg (II)	Co (II)	Ni (II)	Mo (VI)	Zn (II)	Ca (II)	Sn (II)	Pb (II)	Bi (III)	Hg (II)	Cd (II)	Al (III)	Sb (III)
T_L	14	4.5	50	14	15	10	14	40	2	10	10	8	15	10	8
Log K_s	7.15	6.6	7.18	7.1	7.1	7.15	7.1	7.17	6.8	6.8	6.4	6.7	7.1	7.0	6.8

Abbreviations: CTAC, cetyltrimethyl ammonium bromide; DDAB, dilauryl dimethyl ammonium bromide; TAAC, tetraamyl ammonium chloride; TEAC, tetraethyl ammonium chloride; SDS, sodium dodecyl sulfate; TX, triton X-100; Oxal., oxalate; Citr., citrate; Tart., tartrate; Phth., phthalate, Acet., acetate.

employed to the 2D and 3D sensors under specific sensing conditions (Fig. 9). No significant change in visible color patterns and in the reflectance spectra of the supermicrosensors were observed (Fig. 9A and B) despite the minimal increase in the reflectance spectra of the supemicrosensors at 450 nm with the addition of the Fe^{3+}, Hg^{2+}, Sn^{2+}, Sb^{3+}, and Bi^{3+} cations. These cations can interfere in the formation [Cu-DZ]$^{n+}$ complex at λ = 450 nm, as proven by the positive errors in the Cu(II) ion-sensing systems (Fig. 9). On the other hand, the addition of Cu(II) analyte to 2D or 3D supermicrosensors showed prominent color changes and enhanced signal intensities, indicating the high binding strength of Cu(II) ion with the DZ-probe at pH 2 compared with the other foreign cations [37]. Moreover, time-dependent studies of the [M-DZ]$^{n+}$ complex formation with the addition of metal ions to DZ-modified supermicrosensors showed faster Cu(II)-to-DZ binding kinetics with the formation of [Cu-$(DZ)_2$]$^{n+}$ complex compared with that of other [M-DZ]$^{n+}$ complex formations at pH 2. The specificity behavior of 2D and 3D supermicrosensors for Cu(II) ions indicate significant ion-selective ability (Fig. 9).

Secondly, the simultaneous selective recognition of Cu(II) ions was tested under controlled sensing experiments. Known concentrations of cations and anions were added to the sensing systems prior the addition of [100 ppb] Cu(II) analyte ions. The competing effects of the actively diverse cations and anions at pH 2 are shown in Table 2. Despite the slight decrease in tolerance concentration (Table 2 vs. Fig. 8), the tolerance towards cations, complexants, and surfactants showed satisfactory findings. However, the UV/Vis reflectance spectra of the [Cu-$(DZ)_2$]$^{n+}$ complex varied within a permissible tolerance limit of ±5% (Fig. 8, dotted curve), indicating high thermodynamic Cu (II)-to-DZ ligand binding. Most electrolyte species, surfactants, and complexing agents have no effect on Cu(II) complex formations. However, the presence of Cl^- and SO_4^{2-} electrolyte species appeared to decrease slightly the binding strength between Cu(II) and DZ-probe, as shown by the log K_s values (Table 2). The competing effects of the other interfering cations with Cu(II) ion-sensors showed a different trend. Metal ions like Fe^{3+}, Hg^{2+}, Sn^{2+}, Sb^{3+}, and Bi^{3+} competed effectively with Cu(II) ion. These interfering cations showed severe interference at high loading levels, providing positive errors in the Cu(II) ion-sensing systems, as shown by the decrease in the binding strength of the [Cu-$(DZ)_2$]$^{n+}$ complex. Despite the competing effects of such interfering ions on Cu(II) ion binding at pH 2, the time-dependent studies of the [Cu-$(DZ)_2$]$^{n+}$ complex in the presence of interfering cations showed that the Cu(II)-to-DZ binding was stable for a month or even longer. To counteract such disturbance, we added (0.05 M) NH_4F, oxalate, citrate, thiosulfate, and tartrate under specific sensing conditions in order to enhance the tolerable concentration of active Fe^{3+}, Hg^{2+}, Sn^{2+}, Sb^{3+}, and Bi^{3+} ions, respectively (Table 2). The active interfering cations exhibited strong preference with such ligands, thereafter forming inner-sphere complexes and consequently eliminating their effects on Cu(II)-DZ binding (Fig. 8, dotted curve) [42]. The 2D and 3D supermicrosensors showed high selectivity of the Cu(II) analytes even with the presence of real samples containing cations, complexants, and surfactants.

3.6. Analytical applications of the supermicrosensors

The proposed Cu(II) ion-selective method was applied successfully in the determination of Cu(II) ions in some synthetic samples comprising real-life samples such as a wastewater. In this study, simulated multi-component solution containing Cr^{3+}–Fe^{3+} (4 mg/L), Sb^{3+}–Hg^{2+} (8 mg/L), Cd^{2+}–Ni^{2+} (15 mg/L), Co^{2+}–Zn^{2+} (14 mg/L), Ca^{2+}–Mg^{2+} (100 mg/L), PO_4^{3-} (25 mg/L), SO_4^{2-}–SO_3^{2-} (20 mg/L), CH_3COO^-–Cl^- (1000 mg/L), and NO_3^-, CO_3^{2-} (30 mg/L) samples were spiked to a standard solution of Cu(II) (100 μg/L). The determination of Cu(II) ions was visualized with the naked eye (Scheme 1) and quantitatively determined by UV analysis at λ = 450 nm. The quantification data of the Cu(II) ion sample examined 10 times were fitted in the calibration plot (Fig. 8). The calibrated concentration of Cu(II) ion in these multi-component samples was 100.6 ± 0.4 μg/L with a confidence level of 99% and relative standard deviation of 5%. Despite the competing effects of the interfering species, particularly when certain species existed in the multi-component system with high concentration, the good agreement between the analytical results indicate the successful applicability of the proposed method in determining Cu(II) ions in the presence of various interfering cations and anions. The more extensive analytical results indicate that the use of the supermicrosensor as Cu(II) ion strips for field screening can be a time- and cost-alternative tool to current effective laboratory assays.

4. Conclusion

2D and 3D supermicroporous carriers have enabled the construction of high sensitive responses with easily modified, selective, and sensitive recognition of Cu(II) target ions down to subnanomolar concentrations (~10^{-9} mol/dm^3). Rapid kinetic assessments in the order of seconds were obtained without employing sophisti-

cated instruments. The potential use of ordered supermicropores as selective shape and size carriers to accommodate hydrophobic chromophore molecules such as DZ-probe have led to significant signal transduction of chemosensors in response to Cu(II)-DZ binding events. Among all 2D and 3D supermicropore chemosensors, the 3D cubic *Fd3m* chemosensors exhibited easy ion transport and high affinity binding events, particularly at the trace level of target ions. The more extensive analytical results indicate successful applicability of the supermicrosensors under the proposed sensing condition in determining Cu(II) ions in the presence of various interfering cations and anions. The supermicrosensor can serve as a potential candidate for environmental monitoring, test strips, and pollution control.

Acknowledgement

The authors acknowledge the University of Tanta, Egypt for granting leave of absence for Sherif El-Safty.

References

[1] C.T. Kresge, M.E. Leonowicz, W.J. Roth, J.C. Vartuli, J.S. Beck, Nature 359 (1992) 710.
[2] (a) D. Zhao, Q. Huo, F. Jianglin, B.F. Chmelka, G.D. Stucky, J. Am. Chem. Soc. 120 (1998) 6024;
(b) C. Yu, B. Tian, J. Fan, G.D. Stucky, D. Zhao, J. Am. Chem. Soc. 124 (2002) 4556.
[3] (a) P.T. Tanev, T.J. Pinnavaia, Science 267 (1995) 865;
(b) S.A. Bagshaw, E. Prouzet, T.J. Pinnavaia, Science 269 (1995) 1242.
[4] (a) S. Che, A.E. Garcia-Bennett, T. Yokoi, K. Sakamoto, H. Kunieda, O. Terasaki, T. Tatsumi, Nat. Mater. 2 (2003) 801;
(b) S. Inagaki, S. Guan, T. Ohsuna, O. Terasaki, Nature 416 (2002) 304.
[5] (a) S.A. El-Safty, J. Porous Mater. (2010), doi:10.1007/s10934-0109390-4;
(b) S.A. El-Safty, J. Porous Mater. 15 (2008) 369–387.
[6] (a) G.S. Attard, J.C. Glyde, C.G. Göltner, Nature 378 (1995) 366;
(b) C.G. Göltner, S. Henke, M.C. Weissenberger, M. Antonietti, Angew Chem. Int. Ed. 37 (1998) 613;
(c) P. Feng, X. Bu, G.D. Stucky, D.J. Pin, J. Am. Chem. Soc. 122 (2000) 994.
[7] (a) S.A. El-Safty, T. Hanaoka, F. Mizukami, Adv. Mater. 17 (2005) 47;
(b) S.A. El-Safty, F. Mizukami, T. Hanaoka, J. Phys. Chem. B 109 (2005) 9255;
(c) S.A. El-Safty, F. Mizukami, T. Hanaoka, J. Mater. Chem. 15 (2005) 2590;
(d) S.A. El-Safty, Y. Kiyozumi, T. Hanaoka, F. Mizukami, J. Phys. Chem. 112 (2008) 5476.
[8] (a) A. Corma, Chem. Rev. 97 (1997) 2373;
(b) S.A. El-Safty, Y. Kiyozumi, T. Hanaoka, F. Mizukami, Appl. Catal. B: Environ. 82 (2008) 169–179.
[9] (a) J. Fan, C. Yu, J. Lei, B. Tian, L. Wang, Q. Luo, B. Tu, W. Zhou, D. Zhao, Angew. Chem. Int. Ed. 42 (2003) 3146;
(b) S.A. El-Safty, A. Shahat, W. Warkocki, M. Ohnuma, Small, doi:10.1002/smll.201001303.
[10] (a) S.A. El-Safty, M.A. Mekawy, A. Yamaguchi, A. Shahat, K. Ogawa, N. Teramae, Chem. Commun. 46 (2010) 3917;
(b) A.B. Desacalzo, K. Rurack, H. Weisshoff, R.M. Manez, M.D. Marcos, P. Amoros, K. Hoffmann, J. Soto, J. Am. Chem. Soc. 127 (2005) 184;
(c) J. Liu, Y. Lu, J. Am. Chem. Soc. 126 (2004) 12298;
(d) M.C. Aragoni, M. Arca, F. Demartin, F.A. Devillanova, F. Isaia, A. Garau, V. Lippolis, F. Jalali, U. Papke, M. Shamsipur, L. Tei, A. Yari, G. Verani, Inorg. Chem. 41 (2002) 6623;
(e) S.A. El-Safty, A. Shahat, M.A. Mekawy, H. Nguyen, W. Warkocki, M. Ohnuma, Nanotechnology 21 (2010) 375603.
[11] (a) R. Ryoo, I.S. Park, S. Jun, C.W. Lee, M. Kruk, M. Jaroniec, J. Am. Chem. Soc. 123 (2001) 1650;
(b) S.A. Bagshaw, A.R. Hayman, Adv. Mater. 13 (2001) 1011;
(c) Y. Zhou, M. Antonietti, Adv. Mater. 15 (2003) 1452;
(d) M. Polverejan, Y. Liu, T.J. Pinnavaia, Chem. Mater. 14 (2002) 2283.
[12] (a) Y. Di, X. Meng, L. Wang, S. Li, F.S. Xiao, Langmuir 22 (2006) 3068;
(b) E. Prouzet, T.J. Pinnavaia, Angew. Chem. Int. Ed. 36 (1997) 516;
(c) S. Che, Y. Sakamoto, O. Terasaki, T. Tatsumi, Chem. Mater. 13 (2001) 2237;
(d) L. Beaudet, K.Z. Hossain, L. Mercier, Chem. Mater. 15 (2003) 327.
[13] (a) M. Kruk, T. Asefa, M. Jaroniec, G.A. Ozin, J. Am. Chem. Soc. 124 (2002) 6383;
(b) Z. Wang, J.M. Heising, A. Clearfield, J. Am. Chem. Soc. 125 (2003) 10375.
[14] (a) B.G. Shpeizer, V.I. Bakhmutov, A. Clearfield, Micropor. Mesopor. Mater. 90 (2006) 81;
(b) B.G. Shpeizer, A. Clearfield, J.M. Heising, Chem. Commun. (2005) 2396.
[15] (a) P. Buhlmann, E. Pretsch, E. Bakker, Chem. Rev. 98 (1998) 1593;
(b) P. Chen, C. He, J. Am. Chem. Soc. 126 (2004) 728;
(c) L.B. Desmonts, J. Beld, R.S. Zimmerman, J. Hernando, P.M. Mary, F.G. Parajo, N.F. van Hulst, A.V. den Berg, D.N. Reinhoudt, M.C. Calama, J. Am. Chem. Soc. 126 (2004) 7293;
(d) M. Boiocchi, M. Bonizzoni, L. Fabbrizzi, G. Piovani, A. Taglietti, Angew. Chem. Int. Ed. 43 (2004) 3847;
(e) M. Comes, G.R. Lopez, M.D. Marcos, R.M. Manez, F. Sancenon, J. Soto, L.A. Villaescusa, P. Amoros, D. Beltran, Angew. Chem. Int. Ed. 44 (2005) 2918;
(f) B. Maa, S. Wua, F. Zenga, Sens. Actuators B 145 (2010) 451;
(g) B.N. Ahamed, I. Ravikumar, P. Ghosh, New J. Chem. 33 (2009) 1825.
[16] (a) J.S. Lee, M.S. Han, C.A. Mirkin, Angew. Chem. Int. Ed. 46 (2007) 4093;
(b) J.M. Nam, C.S. Thaxton, C.A. Mirkin, Science 301 (2003) 1884;
(c) B. Lei, B. Li, H. Zhang, S. Lu, Z. Zheng, W. Li, Y. Wang, Adv. Funct. Mater. 16 (2006) 1883;
(d) S. Isik, W. Schuhmann, Angew. Chem. Int. Ed. 45 (2006) 7451–7454;
(e) S. Yoon, A.E. Alers, A.P. Wong, C.J. Chang, J. Am. Chem. Soc. 127 (2005) 16030;
(f) P. Zuo1, B.C. Yin1, B.C. Ye, Biosens. Bioelectron. 25 (2009) 935.
[17] (a) G. Wirnsberger, B.J. Scott, G.D. Stucky, Chem. Commun. (2001) 119;
(b) L. Nicole, C. Boissiere, D. Grosso, P. Hesemann, J. Moreau, C. Sanchez, Chem. Commun. (2004) 2312.
[18] (a) T. Balaji, S.A. El-Safty, H. Matsunaga, T. Hanaoka, F. Muzukami, Angew. Chem. Int. Ed. 45 (2006) 7202;
(b) S.A. El-Safty, A.A. Ismail, H. Matsunaga, F. Muzukami, Chem. Eur. J. 13 (2007) 9245;
(c) S.A. El-Safty, D. Prabakaran, A.A. Ismail, H. Matsunaga, F. Mizukami, Adv. Funct. Mater. 17 (2007) 3731;
(d) S.A. El-Safty, A.A. Ismail, H. Matsunaga, F. Muzukami, J. Phys. Chem. C 112 (2008) 4825;
(e) S.A. El-Safty, D. Prabhakaran, A.A. Ismail, H. Matsunaga, F. Muzukami, Chem Mater. 20 (2008) 2644;
(f) S.A. El-Safty, Adsorption 15 (2009) 227.
[19] (a) M. Comes, M.D. Marcos, F. Sancenon, J. Soto, L.A. Villaescusa, P. Amoros, D. Beltran, Adv. Mater. 16 (2004) 1783;
(b) A.B. Desacalzo, K. Rurack, H. Weisshoff, R.M. Mártinez-Mánez, M.D. Marcos, P. Amoros, K. Hoffmann, J. Soto, J. Am. Chem. Soc. 127 (2005) 184;
(c) T. Balaji, M. Sasidrharan, H. Matsunaga, Analyst 130 (2005) 1162;
(d) R. Metivier, I. Leray, B.D. Lebeau, B. Valeur, J. Mater. Chem. 15 (2005) 2965;
(e) S.A. El-Safty, D. Prabhakaran, Y. Kiyozumi, F. Mizukami, Adv. Funt. Mater. 18 (2008) 1739;
(f) S.A. El-Safty, A.A. Ismail, T. Hanaoka, H. Matsunaga, F. Mizukami, Adv. Funct. Mater. 18 (2008) 1485;
(g) S.A. El-Safty, J. Mater. Sci. 44 (2009) 6764.
[20] (a) C.F. Chow, M.H.W. Lam, W.Y. Wong, Inorg. Chem. 43 (2004) 8387;
(b) J.V.R. Lis, M.D. Marcos, R.M. Mánez, K. Rurack, J. Soto, Angew. Chem. Int. Ed. 44 (2005) 4405.
[21] (a) S.J. Lee, S.S. Lee, J.Y. Lee, J.H. Jung, Chem. Mater. 18 (2006) 4713;
(b) J. Liu, Y. Lu, Chem. Mater. 16 (2004) 3231;
(c) M. Telting-Diaz, E. Barkker, Anal. Chem. 74 (2002) 5251;
(d) W. Yantase, C. Timchalk, G.F. Fryxell, B.P. Dockendorff, Y. Lin, Talanta 68 (2005) 256;
(e) V.K. Gupta, A.K. Jain, P. Kumar, Sens. Actuators B 120 (2006) 259;
(f) M. Schmittel, H.W. Lin, Angew. Chem. Int. Ed. 45 (2006) 1–5;
(g) T. Gunnlaugsson, J.P. Leonard, N.S. Murray, Org. Lett. 10 (2004) 1557;
(h) F. Yu, W. Zhang, P. Li, Y. Xing, L. Tong, J. Ma, B. Tang, Analyst 134 (2009) 1826.
[22] (a) A. Morrow, G. Witshire, A. Huvsthous, At. Spectrosc. 18 (1997) 23;
(b) M.V. Hinds, D.C. Gregoie, E.A. Ozaki, J. Anal. At. Spectrom. 12 (1997) 131;
(c) Y. Yamini, M. Chaloosi, H. Ebrahimzadeh, Talanta 56 (2002) 797;
(d) X.J. Feng, B. Fu, Anal. Chim. Acta 371 (1998) 109;
(e) P. Ostapczuk, Anal. Chim. Acta 273 (1993) 35;
(f) T. Ferri, S. Paci, R. Morabito, Ann. Chim. 86 (1996) 595;
(g) M.H.P. Azar, D. Djozan, H. mohammad, Anal. Chim. Acta 437 (2001) 217;
(h) M. Koneswaran, R. Narayanaswamy, Sens. Actuators B 139 (2009) 104.
[23] (a) C. Vulpe, B. Levinson, S. Whiteny, S. Packman, J. Gitschier, Nat. Genet. 3 (1993) 7;
(b) P.C. Bull, G.R. Thomas, J.M. Rommens, J.R. Forbes, D.W. Cox, Nat. Genet. 5 (1993) 327.
[24] (a) J.E. Tahan, R.A. Romeo, Anal. Chim. Acta 273 (1993) 53;
(b) P.L. Malvankar, V.M. Shinde, Analyst 116 (1991) 1081.
[25] A.J. Tong, Y. Akama, S. Tanaka, Analyst 115 (1990) 947.
[26] Y.H. Tian, R. Pipalnik, H.V. Fanger, J. Radioanal. Nucl. Chem. 139 (1990) 43.
[27] Z. Fang, S. Xu, S. Zhang, Anal. Chim. Acta 164 (1984) 41.
[28] E.A.G. Zagatto, A.O. Jacintho, F.F.J. Krug, B.F. Reis, R.E. Bruns, M.C.U. Araujo, Anal. Chim. Acta 145 (1983) 169.
[29] A. Hu, R.E. Dessy, A. Graneli, Anal. Chem. 55 (1983) 320.
[30] G. Gillain, G. Duyckaerts, A. Disteche, Anal. Chim. Acta 106 (1979) 23.
[31] O.W. Lau, S.Y. Ho, Anal. Chim. Acta 280 (1993) 269.
[32] V. Rigin, Anal. Chim. Acta 283 (1993) 895.
[33] (a) L. Mei, Y. Xiang, N. Li, A. Tong, Talanta 72 (2007) 1717;
(b) B.R. White, J.A. Holcombe, Talanta 71 (2007) 2015;
(c) A. Yari, N. Afshari, Sens. Actuators B 119 (2006) 531;
(d) T. Leelasattarathkul, S. Liawruangrath, M. Rayanakorn, B. Liawruangrath, W. Oungpipat, N. Youngvises, Talanta 72 (2007) 126;
(e) Y. Zheng, X. Cao, J. Orbulescu, V. Konka, F.M. Andreopoulos, S.M. Pham, R.M. Leblance, Anal. Chim. Acta 75 (2003) 1706;
(f) M. Arduini, S. Marcuz, M. Montolli, E. Rampazzo, F. Mancin, S. Gross, L. Armelao, P. Tecilla, U. Tonellato, Langmuir 21 (2005) 9314.
[34] F.-J. Huo, J. Su, Y.-Q. Sun, C.-X. Yin, H.-B. Tong, Z.-X. Nie, Dyes Pigm. 86 (2010) 50.
[35] (a) T. Shtoyko, S. Conklin, A.T. Maghasi, J.N. Richardson, A. Piruska, C.J. Seliskar, W.R. Heineman, Anal. Chem. 76 (2004) 1466;

(b) A.K. Singh, S. Mehtab, A.K. Jain, Anal. Chim. Acta 575 (2006) 25.
[36] (a) L.K. Chau, P. Tien, Chem. Mater. 11 (1999) 2141;
(b) G.G. Huang, J. Yang, Anal. Chem. 75 (2003) 2262;
(c) J. Baffle, J. Ueberfeld, N. Parthasarathy, Anal. Chem. 74 (2002) 664.
[37] (a) A.P. Argekar, A.K. Shetty, Analyst 120 (1995) 1819;
(b) G. Gumus, H. Filik, B. Demirata, Anal. Chim. Acta 547 (2005) 138;
(c) P.A. Jeronimo, A.N. Araujo, M.C. Montenegro, D. Satinsky, P. Solich, Anal. Chim. Acta 504 (2004) 235;
(d) W. Ngeontae, W. Aeungmaitrepirom, T. Tuntulani, Talanta 71 (2007) 1075;
(e) Y. Zheng, X. Cao, J. Orbulescu, V. Konka, F.M. Andreopoulos, S.M. Pham, R.M. Leblanc, Anal. Chem. 75 (2003) 1706.
[38] (a) A. Safavi, M. Bagheri, Sens. Actuators B 99 (2004) 608;
(b) A.A Ensafi, M. Fouladgar, Sens. Actuators B 113 (2006) 88;
(c) O.S. Wolfbeis, J. Mater. Chem. 15 (2005) 2657;
(d) S.A. Asher, A.C. Sharma, A.V. Goponenko, M.M. Ward, Anal. Chem. 75 (2003) 1676.
[39] (a) M.R. Jamali, Y. Assadi, F. Shemirani, M.R.M. Hosseini, R.R. Kozani, M.M. Farahani, M.S. Niasari, Anal. Chim. Acta 579 (2006) 68;
(b) E. Kendüzler, A.R. Türker, O. Yalcinkaya, Talanta 69 (2006) 835.
[40] (a) E. Palomares, R. Vilar, A. Green, J.R. Durrant, Adv. Funct. Mater. 2 (2004) 111;
(b) A.M. Liu, K. Hidajat, S. Kawi, D.Y. Zhao, Chem. Commun. (2000) 1145;
(c) R.T. Bronson, M. Montalti, L. Prodi, N. Zaccheroni, R.D. Lamb, N.K. Dalley, R.M. Izatt, J.S. Bradshaw, P.B. Savage, Tetrahedron 60 (2004) 11139;
(d) J. Kawakami, R.T. Bronson, G. Xue, J.S. Bradshaw, R.M. Izatt, P.B. Savage, Supramol. Chem. 1 (2003) 221.
[41] (a) D.S. Koktysh, X.R. Liang, B.G. Yun, I.P. Santos, R.L. Matts, M. Giersig, C.S. Rodriguez, L.M.L. Marzan, N.A. Kotov, Adv. Funct. Mater. 12 (2002) 225;
(b) R. Kramer, Angew. Chem. Int. Ed. 37 (1998) 772;
(c) Y.Q. Weng, Y.L. Teng, F. Yue, Y.R. Zhong, B.H. Ye, Inorg. Chem. Commun. 10 (2007) 443.
[42] (a) J.A. Broomhead, J. Chem. Soc. (1971) 645;
(b) C.A. Bunton, J.H. Carter, D.R. Lieweellyn, C. O'Connor, A.L. Odell, Y. Yih, J. Chem. Soc. (1964) 4615;
(c) N. Serpone, D.G. Bickley, Prog. Inorg. Chem. 71 (1971) 391.